Emergent orbital-selective many-body effects upon doping strained graphene

L. Craco
Institute of Physics, Federal University of Mato Grosso, 78060-900 Cuiabá, MT, Brazil
and Leibniz Institute for Solid State and Materials Research Dresden, D-01069 Dresden, Germany

(Received 1 December 2020; revised 8 February 2021; accepted 9 February 2021; published 19 February 2021)

We explore the effect of doping on the correlated electronic structure of strained graphene. It is shown that the interplay between sizable multiorbital Coulomb interactions and electron-hole doping induces an orbital-selective electronic state, characterized by the coexistence of π-band Dirac-Kondo quasiparticles and emergent σ-band metallicity. The underlying orbital selectivity in the presence of spin-polarized electron bands, relevant to experiments of strained graphene proximitized to magnetic ions, shows coexistent Mott-localized and semimetal electronic states with, respectively, π- and σ-orbital character. Our results provide the theoretical foundations for understanding the intricate and interdependent changes in orbital degrees of freedom in strained carbon-based materials, and they open up an avenue to systematic studies of quantum many-body effects in correlated Dirac fermion systems.

DOI: 10.1103/PhysRevB.103.075135

I. INTRODUCTION

Graphene [1], a honeycomb monolayer of carbon atoms, is a prototype of the layered class of Dirac materials [2]. The low-energy excitations of pristine graphene can be described as massless Dirac fermions, as the electronic spectrum is linear in a single-particle picture. As such, graphene hosts chiral Dirac fermions and mimics the physics of quantum electrodynamics in a solid-state environment [1,3]. Importantly, due to its intrinsic mechanical and electronic properties, graphene might be a way to realize transparent, flexible-stretchable electronics [4,5]. In any case, the interest in graphene goes well beyond the distinctive behavior of its low-energy excitations, which are protected against many-particle interactions [6], particularly when considering the combined effect of strain engineering [7,8] and many-body electron-electron interactions [9], where the massless Dirac bands are predicted to be reshaped [10,11] due to strain-induced one-particle band narrowing [12].

Many-body interactions can lead to renormalizations in the band structure, such that strongly correlated ground states might develop in strained [10,11,13] as well as in doped graphene [14–17]. In the case of doped graphene, the van Hove singularity in the density-of-states (DOS) of graphene's π-band has recently reached the Fermi level, E_F [18]. More precisely, upon tuning the doping level of graphene, flatbands, connecting the high-symmetry points K and K' of graphene's Brillouin zone [14], develop at E_F. There, the DOS diverges and the excess charge carriers enhance both electronic correlations [16,17] as well as electron-phonon coupling [16,19]. Similar effects have been observed in strongly correlated systems [20], and they are now commonly referred to as extended van Hove singularity [14]. Angle-resolved photoelectron spectroscopy (ARPES) in n-doped epitaxial graphene on SiC [17] reveals the shrinking of the π^* hole pocket, providing evidence for the emergence of the Lifshitz transition in doped graphene. Importantly, this transition is found to be driven by electronic structure renormalizations rather than a rigid band shift [17], confirming the importance of many-body interactions in the vicinity of the van Hove singularities.

Taken together, experimentally there are two feasible routes to enlarging the concentration of states, thus enhancing many-body interactions in graphene [18], namely via tuning the doping level in the vicinity of the van Hove singularity [14–17], or via strain-induced one-particle narrowing [11–13]. However, despite the broad experimental and theoretical understanding of the physical properties of normal, strained, and doped graphene, the electronic structure reconstruction driven by the interplay between electron-electron interactions [21], electron-hole doping [22], and strain [12] remains an open issue of fundamental and applied importance. Motivated by this open issue, we report here a local density approximation plus dynamical mean-field theory (LDA + DMFT) [23] study on strained graphene to demonstrate the emergence of collective states associated with a many-body, correlated electron phenomenon. Excitingly, our theoretical predictions for doped-strained graphene include exotic low-energy electronic states, such as Dirac-Kondo quasiparticles [24], as well as the coexistence of π-Mott localized [11] and semimetallic electronic states with σ-band character.

In recent years, there have been considerable efforts to explore the possibility of tuning the physical properties in graphene by applying mechanical strain for experimental [4,25] and theoretical [26–29] interests. Theoretically, at the one-particle level strain can turn graphene metallic [12]. With this in place, in earlier studies we explored the physical properties of graphene when its hexagonal lattice is stretched out of equilibrium [10,11,13]. In particular, motivated by a scanning tunneling microscopy (STM) experiment probing the low-energy electronic structure of highly strained graphene nanobubbles [8], we have carried out LDA + DMFT calculations to study the electronic structure evolution induced

by multiorbital (MO) electronic interactions in 30% isotropically strained graphene [10]. To advance our understanding of the electronic structure reconstruction due to intrinsic many-particle electron-electron interactions [9], here we report LDA + DMFT results upon tuning the doping level of highly strained graphene [10].

II. METHOD

In this work, we explore the effect of doping on the electronic structure reconstruction of 30% strained graphene [4,12,26]. Similar to Refs. [10,11,13], here we perform density functional theory plus dynamical mean-field theory (DFT + DMFT) calculations [23], showing the emergent electronic state associated with the interplay between (electron/hole) doping and MO electron-electron interactions at currently acceptable strain conditions [4]. Within our self-consistent DFT + DMFT scheme, we use the orbital-resolved LDA DOS for 30% [12] strained graphene computed in Ref. [10] as the bare on-particle input to MO-DMFT. However, for the sake of clarity, we shall notice that the bare one-particle electronic properties of the normal and 30% strained (lattice constant of $L = 0.3209$ nm) [12] graphene were investigated in Ref. [10] within DFT, as implemented in the SIESTA simulation package [30]. We used the LDA to DFT with the Ceperley-Alder [31] exchange-correlation functional and norm-conserving Troullier-Martins pseudopotentials [32]. The charge density was represented on a real-space grid with an energy cutoff of 200 Ry. The reciprocal space was sampled with a fine $180 \times 1 \times 180$ Monkhorst-Pack k-point grid [33].

As shown in earlier DFT studies [10–12], the linear (Dirac-like) band dispersion of unstrained graphene is reshaped by isotropically increasing the lattice constant L of graphene. A sizable reduction of the one-electron bandwidth W, including the energy position of the van Hove singularities at the border of the Dirac dispersion, is found in the p_z band for the lattice constants varying from 0.246 69 to 0.3209 nm [10,12]. Also interesting is the band-structure reconstruction within the planar $p_{x,y}$ bands, where the charge gap shrinks upon increasing the lattice constant until it is fully suppressed at large L [11,12]. This in turn suggests accessibility of engineering tunable electronic states in superstrained [11] graphenelike systems.

The many-body Hamiltonian relevant to strained graphene [10,11,13] reads $H = \sum_{\mathbf{k}a\sigma} \epsilon_a(\mathbf{k}) c^\dagger_{\mathbf{k}a\sigma} c_{\mathbf{k}a\sigma} + U \sum_{ia} n_{ia\uparrow} n_{ia\downarrow} + \sum_{ia\neq b} U' n_{ia} n_{ib} - J_H \sum_{ia\neq b} \mathbf{S}_{ia} \cdot \mathbf{S}_{ib}$, where $a = x, y, z$ label the diagonalized p-bands, and $\epsilon_a(\mathbf{k})$ is the one-electron band dispersion, which encodes details of the actual one-electron band structure of strained graphene. $U' \equiv U - 2J_H$, with U, U' being the intra- and interorbital Coulomb repulsion and J_H is the Hund's rule coupling [34]. Here, we perform MO LDA + DMFT [23] calculations for the three-orbital model of strained graphene, showing the effect of electron/hole doping [22] as well as strong MO electronic renormalizations induced by spin splitting [16] when approaching the extended van Hove singular limit [14], using the MO iterated-perturbation-theory (MO-IPT) as an impurity solver for DMFT. The detailed formulation of MO-IPT for correlated electron systems has already been developed [35] and used to describe the physical properties of broad s- [36] and p-band [37,38] materials, so we do not repeat the equations here.

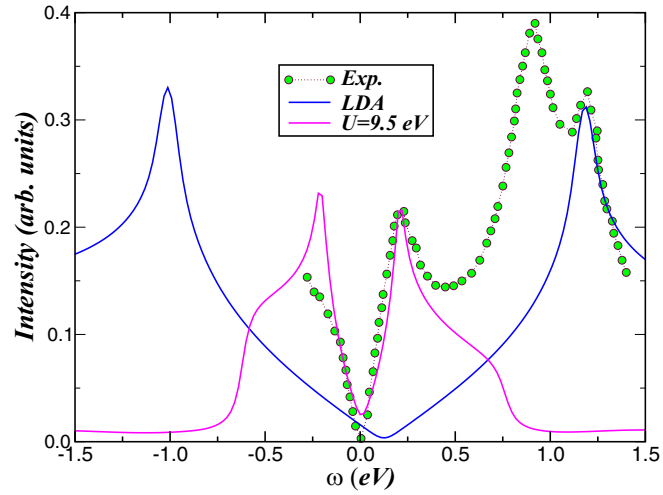

FIG. 1. Theory-experiment comparison between scanning tunneling microscopy data on strained graphene nanobubbles grown on the Pt(111) surface [8], LDA, and LDA + DMFT ($U = 9.5$ eV) spectral functions of 30% strained graphene [10], showing good agreement at high and low energies, respectively.

III. RESULTS AND DISCUSSION

A. Electronic structure of 30% strained graphene

For a proof-of-concept demonstration, in Fig. 1 we display the reconstructed electronic structure of 30% ($L = 0.3209$ nm) strained graphene [10]. As can be seen, the LDA + DMFT result for $U = 9.5$ eV captures important low-energy features probed in scanning tunneling experiments [8], providing a quantitative account for many-body effects as well as a proof of principle for engineering Dirac-Kondo quasiparticles [24] in correlated hexagonal systems. In particular, without assuming Landau levels arising from strain-induced pseudomagnetic fields [5,8] as well as bond stretching and bond bending effects [39], it is realized that in highly strained graphene, the interplay between electron-electron interactions [9] and strain-induced one-particle band narrowing is a step toward realizing exotic electronic states, with prominent Dirac-Kondo quasiparticles at low temperatures, which can be tested in future studies on stretched hexagonal lattice systems.

As seen in Fig. 1, the energy-dependence of one representative current-voltage curve at low energies is quantitatively well described using LDA + DMFT spectral functions with $U = 9.5$ eV [9]. As reported in Ref. [10], our theory-experiment comparison in Fig. 1 suggests that the tunneling experiment is mainly probing out-of-plane electronic states. This in turn suggests that the shape and the width of the low-energy differential tunneling conductance (dI/dV) are well accounted for by the emergence of Dirac-Kondo quasiparticles [24] in strained graphene. As can be seen, the V-shaped band dispersion and the position of the Dirac-band edge above E_F are well reproduced by LDA + DMFT. However, in spite of good agreement at low energies, the discrepancy between

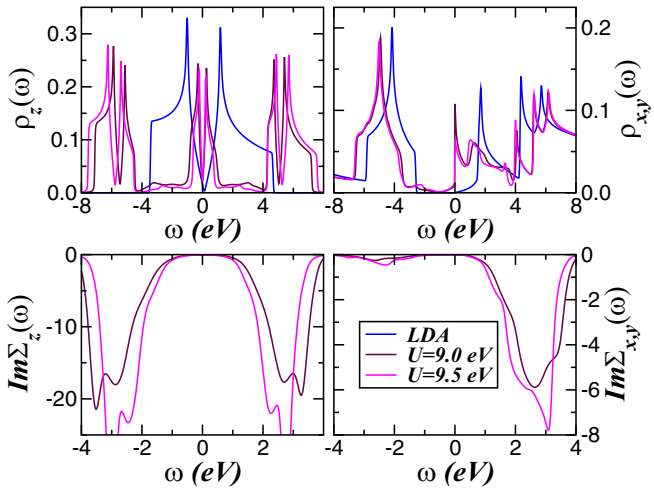

FIG. 2. LDA + DMFT orbital-resolved spectral functions and self-energy imaginary parts of 30% strained graphene. Particularly relevant features are the narrow Dirac-Kondo quasiparticles and the downshift as compared to the LDA of the p_z and $p_{x,y}$ electronic states, respectively.

the LDA + DMFT electronic spectra derived for $U = 9.5$ eV [10] and experiment above 0.4 eV might be due to tip [40] or to bond stretching and bond bending [39] effects not included in our theory. An additional source of discrepancy might also be related to nonlocal (i.e., near neighbor) linear contributions to dI/dV coming from less correlated π orbitals close to the tip. This is reflected by the good theory-experiment agreement between the van Hove singularity of the LDA DOS and the peak seen at 1.2 eV above E_F in experiment. Taken together, our theory-experiment comparison suggests that the Dirac electrons of neutral graphene might not be completely stable [6] against Coulomb correlation effects. Therefore, upon introducing strong electron-electron interactions [15,16], Dirac-Kondoness [24,38,41] is expected to be seen in strained graphene and related hexagonal p-band materials.

It is now recognized that under external perturbations, the hopping elements are renormalized in nontrivial ways [42]. As mentioned above, in strained graphene an overall reduction of the bare one-electron bandwidth W, including the energy position of the van Hove singularities at the border of the Dirac band dispersion, is obtained for the lattice constant L varying from 0.246 69 to 0.3209 nm [10,12]. As seen in Fig. 1, the electronic states close to the neutrality point, where the LDA DOS vanishes linearly, are shifted to positive energies providing smooth crossover to a metallic state with low carrier density in 30% strained graphene. It is also noteworthy that the energy difference of the two van Hove singularities further decreases with increasing electron-electron correlation effects [10], giving rise to Dirac-Kondo quasiparticles and Hubbard bands with well-defined Dirac-like band dispersions at low and high energies, respectively, as shown in the left upper panel of Fig. 2. It is noteworthy that similar correlated electronic structure reconstruction has recently been derived for the Weyl-Hubbard model treated with the exact diagonalization impurity solver [43], showing as in Fig. 2 that the structure of the Hubbard bands resembles the structure of the original bare DOS. Also interesting in Fig. 2 is the downshift of the conduction-band states of the planar $p_{x,y}$ orbitals. Due to MO electron-electron interactions, the antibonding σ^*-band of 30% strained graphene reaches E_F [10], giving rise to a planar electronic metallic state, as shown in the right upper panel of Fig. 2. Furthermore, dynamical electronic correlations, inducing massive π-band Dirac-Kondo quasiparticles followed by incoherent Hubbard bands, are also encoded in the self-energy imaginary parts, as shown in the left lower panel of Fig. 2. As can be seen, $\mathrm{Im}\Sigma_a(\omega)$ is considerably enhanced with slightly increasing U, particularly within the p_z channel, supporting its strongly correlated Dirac-Kondo nature and its close proximity to Mott localization [11].

B. Filling-controlled electronic structure

Let us now turn to the implications of our LDA + DMFT results upon electron/hole doping strained graphene. However, before delving into this correlated many-particle problem, it should be noted that the partially screened on-site Coulomb interaction parameter for graphene is in the range between 7.62 and 10.16 eV [21]. Due to the good theory-experiment agreement at low energies in Fig. 1, here we chose fixed $U = 9.5$ eV [10] and $J_H = 0.4$ eV [34] values to access many-body effects in doped-strained graphene, which, as shown below, is characterized by reconstructed spectral functions due to large spectral weight transfer (SWT) upon small changes in the total band filling $n_t = n + \delta$, with n being the total p-band occupancy of strained pristine graphene [10].

In Fig. 3 we display the effect of the varying doping level on the electronic structure reconstruction within the weakly carrier doping regime of 30% strained graphene. As expected for strongly correlated electron systems [42], high-energy SWT between the incoherent Hubbard bands is observed in the p_z spectral functions upon small changes in δ. Also interesting is the concomitant shift of the high-energy Dirac-like point energies, which could be probed in future spectroscopy experiments. Interesting as well is the stability of the coherent Dirac-Kondo quasiparticles to small doping, showing almost equal electronic line shape as found in the undoped regime. Similar evolution is also found within the planar orbital sector, showing weak low-energy electronic structure reconstruction due to negligible self-energy corrections (see the low inset of Fig. 3) at low energies. However, as shown below, appreciable electronic renormalization as compared to our results in Fig. 3 is predicted to be seen when pushing E_F [15] of 30% strained graphene in the vicinity of the van Hove singularities.

Figures 4 and 5 highlight the detailed evolution of the correlated spectral functions as a function of electron and hole doping, respectively, for doped strained graphene in the vicinity of the van Hove singularity [15,17]. In both cases, MO dynamical correlations arising from U, U' and J_H lead to SWT over large energy scales upon small changes of carrier doping δ. As can be seen, within the p_z orbital sector, pronounced SWT from the incoherent Hubbard bands above $\omega = \pm 4$ eV to the coherent Dirac-Kondo clouds is obtained in both cases. Also interesting is the particle-hole asymmetry of the self-energy imaginary parts (left lower panels of Figs. 4 and 5), revealing an overall reduction of dynamical

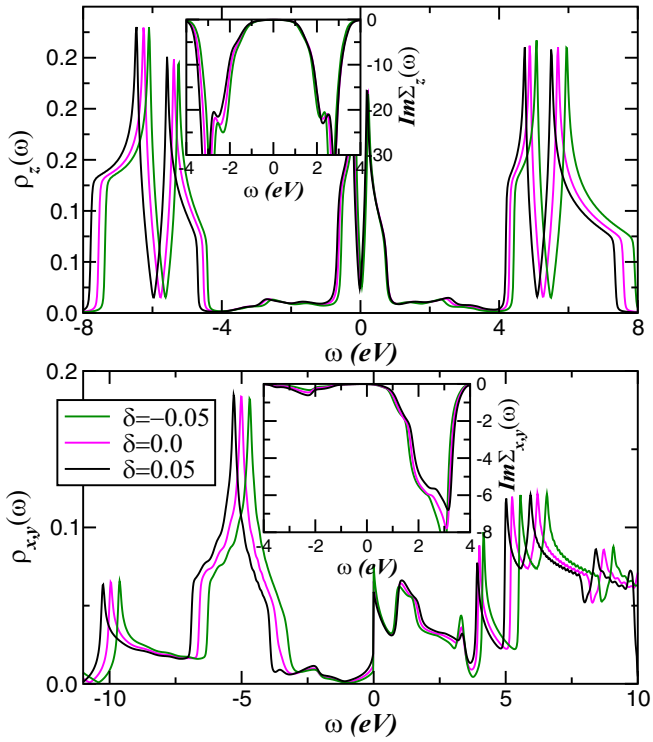

FIG. 3. Comparison between the LDA + DMFT orbital-resolved spectral functions (main panels) and the corresponding self-energy imaginary parts (insets) for the p orbitals of undoped graphene (magenta line) and 30% strained graphene obtained upon electron (black line) and hole (green line) doping. Notice the stability of the low-energy electronic states and the high-energy spectral weight transfer between the Hubbard bands upon small changes of δ.

correlations when the π-band moves away from half-filling with increasing δ. [As a side remark, it should be noted that strong dynamical correlations due to Mott-Hubbard physics is realized close to half-filled systems [42] and increases when approaching this filling, with a corresponding increase of local moments (lower Hubbard bands) in the metallic paramagnetic phase in general.] Remarkable, however, are the differences in SWT observed in the right upper panels of Figs. 4 and 5 as a consequence of strong particle-hole asymmetry of the planar $p_{x,y}$ orbitals. While a lower Hubbard band (LHB) at $\omega \approx 3.5$ eV binding energy is resolved within the $p_{x,y}$ orbital sector for $\delta = -0.2$, the bare σ-bands below -4 eV are almost unaffected by local dynamical correlations upon electron doping strained graphene. Interestingly, in this regime the antibonding σ^*-bands are shifted to lower energies, enhancing σ-band metallicity, as visible in the right upper panel of Fig. 4. Moreover, while the bonding-antibonding band gap is filled up with increasing electron doping, the opposite happens by reducing n_t, implying that electrons and holes behave differently in strained graphene. Future studies are called for to corroborate our prediction for the doping-induced electronic structure reconstruction in highly strained graphene.

Our orbital resolved results in Figs. 4 and 5 are important for understanding the evolution of the Dirac-liquid electronic state of honeycomb lattice systems, showing how the Dirac-Kondo quasiparticles [24] are reshaped by the interplay between MO Coulomb correlations and electron/hole doping within LDA + DMFT. Also relevant in this context is the electronic orbital reconstruction obtained when the doping level is tuned toward the edge of the Dirac band dispersion [14]. Having in mind that the relevance of electron-electron interactions on the electronic structure of doped graphene is quite subtle and not yet completely understood [14–16], in Fig. 6 we display the orbital resolved spectral functions and the corresponding self-energy imaginary parts for δ at the extended van Hove regime, i.e., at δ values where the singularities of the bare LDA DOS reach E_F. As seen, renormalization effects are intrinsically doping-dependent, with electron correlation effects in the p_z orbital being more pronounced upon

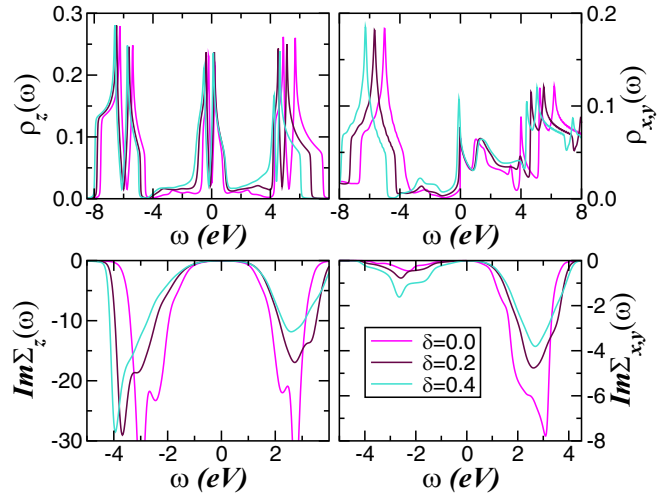

FIG. 4. Effect of electron-doping δ on the LDA + DMFT orbital-resolved spectral functions and the corresponding self-energy imaginary parts for the p orbitals of 30% strained graphene. Notice the high-energy spectral weight transfer and reduced dynamical correlations in the self-energy imaginary parts upon increasing δ.

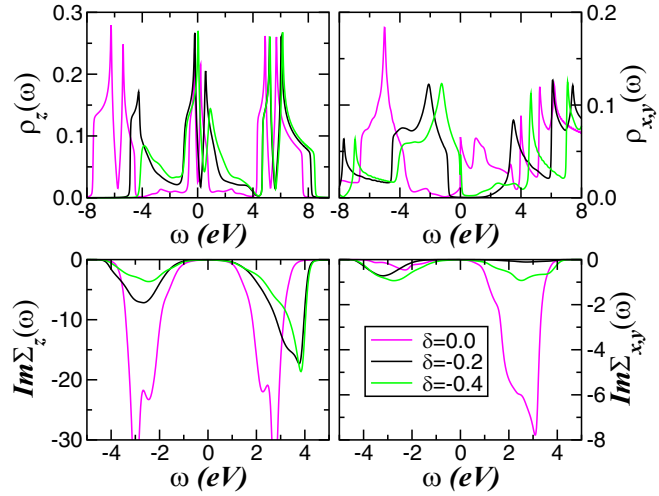

FIG. 5. LDA + DMFT orbital-resolved spectral functions and self-energy imaginary parts for hole-doped ($\delta < 0$) strained graphene. Notice the dynamical transfer of spectral weight in the p_z orbital below the Fermi level and the emergence of lower-Hubbard bands in the correlated semiconductor with $p_{x,y}$ orbital character.

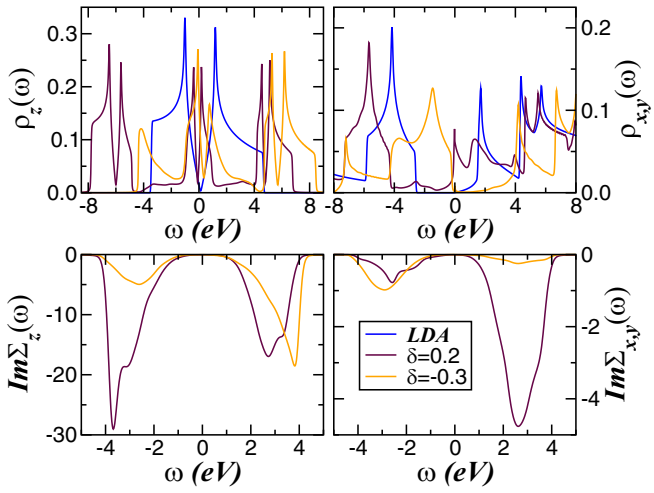

FIG. 6. Effect of electron ($\delta = 0.2$) and hole ($\delta = -0.3$) doping on the LDA + DMFT DOS in the extended van Hove singularity regime of 30% strained graphene, showing stronger multiorbital electron-electron correlation effects upon electron-doping strained graphene.

approaching the singular point via electron doing as a result of large concentration of states in the diverging LDA DOS above E_F of neutral strained graphene. Similar behavior is also seen within the planar orbitals, where the frequency dependence of the self-energy imaginary part above E_F is strongly enhanced above E_F for $\delta = 0.2$ as compared to the hole-doped case. Taken together, our results in Fig. 6 highlight the effect of varying the doping at the level where the bare van Hove singularities coincide with E_F, showing distinctive many-body effects upon electron/hole doping correlated semiconductors and Dirac semimetals. However, whether doped-strained graphene would be unstable to superconducting pairing due to electron-electron interactions [14] remains to be seen in future studies.

C. Spin-split electronic structure

It should be noted that in correlated materials, the competition between kinetic energy and dynamical many-body interactions takes different forms at different energy scales, which might result in an unusual energy dependence of the electronic states upon external perturbations like pressure, doping, and electric and magnetic fields [42]. In correlated MO systems, electron-electron interactions renormalize the DFT + DMFT spectra in two steps near the electronic phase transitions. First, the MO self-energy $[\Sigma_a(\omega)]$ renormalizes the relative band positions depending upon their orbital occupations. The frequency-dependent self-energy causes SWT across large energy scales, drastically modifying the correlated spectral functions. As a consequence of large dynamical SWT, the bare electronic state of strained graphene can be pushed into a Mott localized regime [11] upon increasing the lattice constant of strained graphene from 0.3209 to 0.3759 nm [12]. Below we reveal that upon spin splitting [16], the extended van Hove singularity for $\delta = 0.2$ can host Mott localized p_z electrons coexisting with an emergent σ-band semimetallic state at low energies.

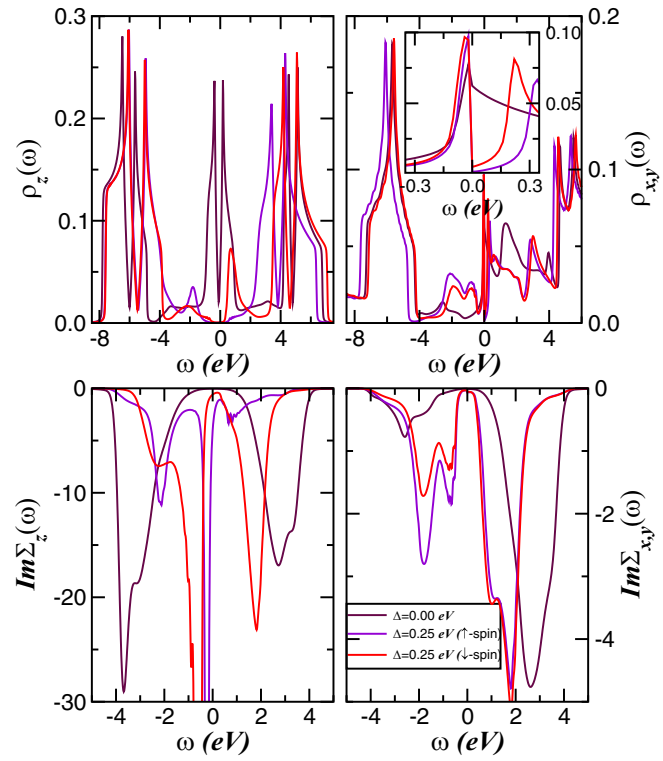

FIG. 7. Effect of lifting the spin degeneracy on the LDA + DMFT spectral function within the van Hove singularity regime of electron-doped ($\delta = 0.2$) strained graphene. Notice the Mott-Hubbard gap in the p_z orbital and the emergence of a correlated semimetallic (see inset) electronic state with $p_{x,y}$-orbital character at low energies.

To provide insights into the spin-split electronic state of strained graphene, we recall here a combined theory-experiment study [16], revealing strong electron correlation effects in graphene by Gd intercalation as well as that the hybridization of graphene with Gd bands pushes the π-band at M close to 0.5 eV below E_F and induces a spin splitting of about 0.5 eV. Motivated thereby, we have performed LDA + DMFT calculations for the spin-split electronic phase [44] of strained graphene at electron doping that coincides with the extended van Hove singularity regime. To proceed, we consider the on-site energy term, $H_\Delta = -\Delta \sum_{i,a}(n_{ia\uparrow} - n_{ia\downarrow})$ in our Hamiltonian H, to simulate the electronic changes induced via the magnetic-proximity effect [16]. Here, Δ acts like an applied uniform magnetic field [45], sensitively controlling the occupations of each orbital in much the same way as the magnetization of a paramagnet as a function of an external Zeeman field. Using a spin splitting $\Delta = 0.25$ eV consistent with experiment [16], the p_z orbital sector is strongly renormalized, giving rise to an overall Mott insulating state. This behavior is encoded by the diverging behavior of the self-energy imaginary part near E_F, as shown in the left lower panel of Fig. 7. In this Mott localized regime, the spectral weight of the coherent Dirac-Kondo quasiparticles is dynamically transferred to the incoherent Hubbard bands at high energies, as expected for strongly correlated electron systems near Mott localization [42]. Although less pronounced, SWT is also visible within the planar $p_{x,y}$ orbitals

of strained graphene, where semimetallic quasiparticles with a narrow and asymmetric line shape emerge at low energies near E_F for $\Delta = 0.25$ eV. Based on our results, in Fig. 7 we predict that similar features would be seen in future strained graphene studies by intercalating Gd [16] or other ions with large magnetic moments.

Finally, it is noteworthy that magnetic impurities in Dirac and Weyl systems exhibit correlated electron physics [41] with distinctive spectroscopic fingerprints. As shown in Fig. 7, the influence of a nearby Mott localized quantum state via a U'-induced strong interorbital proximity effect leads to an unconventional semimetallic electronic state upon lifting the spin degeneracy. Our work, therefore, calls for future studies on doped graphene to reveal orbital-selective Coulomb correlation effects in highly strained graphene [8]. Based on our results, we predict an electronic reconstruction with emergent Mott localized and semimetallic electronic states near the extended van Hove singularity. Characteristic strong correlation features like self-energy corrections and renormalized Dirac-Kondo clouds are all predicted to occur as more and more electrons are transferred onto (or removed from) strained graphene. Observation of dynamical SWT upon doping would constitute microscopic proof of the strongly correlated nature of strained graphene and the importance of treating dynamical correlations adequately to understand unconventional many-particle responses [42].

IV. CONCLUSION

In conclusion, using LDA + DMFT we have explored the electronic structure reconstruction induced by electron/hole doping of highly strained graphene [8]. The interplay between strain-induced one-particle band narrowing and sizable multiorbital electronic correlations drives strained graphene into an orbital-selective metallic regime characterized by narrow π-orbital Dirac-Kondo clouds and a downshift of σ^* states to low energies. Our LDA + DMFT calculations performed within an unbiased unique choice of interaction parameters highlight the role played by electron-band filling and how the proximity to an orbital-selective Mott insulator is a key in determining an emergent semimetallic electronic state in strained graphene with lifted spectral degeneracy. Our microscopic description of coupled multiorbital Hubbard interactions is expected to be a proof of principle for engineering massive Dirac fermions [46] and Weyl-Kondo semimetals [47] in correlated electron systems.

ACKNOWLEDGMENTS

This work is supported by CNPq (Grant No. 304035/2017-3). Acknowledgment is also made to Jörg Fink for discussions as well to CAPES.

[1] K. S. Novoselov, A. K. Geim, S. V. Morozov, D. Jiang, M. I. Katsnelson, I. V. Grigorieva, S. V. Dubonos, and A. A. Firsov, Nature (London) **438**, 197 (2005).
[2] T. O. Wehling, A. M. Black-Schaffer, and A. V. Balatsky, Adv. Phys. **63**, 1 (2014).
[3] A. H. Castro Neto, F. Guinea, N. M. R. Peres, K. S. Novoselov, and A. K. Geim, Rev. Mod. Phys. **81**, 109 (2009); M. I. Katsnelson, Mater. Today **10**, 20 (2009).
[4] K. S. Kim, Y. Zhao, H. Jang, S. Y. Lee, J. M. Kim, K. S. Kim, J.-H. Ahn, P. Kim, J.-Y. Choi, and B. H. Hong, Nature (London) **457**, 706 (2009).
[5] Y. Jiang, J. Mao, J. Duan, X. Lai, K. Watanabe, T. Taniguchi, and E. Y. Andrei, Nano Lett. **17**, 2839 (2017), and references therein.
[6] I. S. Tupitsyn and N. V. Prokof'ev, Phys. Rev. Lett. **118**, 026403 (2017).
[7] C. Si, Z. Sun, and F. Liu, Nanoscale **8**, 3207 (2016).
[8] N. Levy, S. A. Burke, K. L. Meaker, M. Panlasigui, A. Zettl, F. Guinea, A. H. Castro Neto, and M. F. Crommie, Science **329**, 544 (2010).
[9] T. O. Wehling, E. Şaşıoğlu, C. Friedrich, A. I. Lichtenstein, M. I. Katsnelson, and S. Blügel, Phys. Rev. Lett. **106**, 236805 (2011).
[10] L. Craco, D. Selli, G. Seifert, and S. Leoni, Phys. Rev. B **91**, 205120 (2015).
[11] L. Craco, S. S. Carara, and S. Leoni, Phys. Rev. B **94**, 165168 (2016).
[12] G. Gui, J. Li, and J. Zhong, Phys. Rev. B **78**, 075435 (2008).
[13] L. Craco, Phys. Rev. B **96**, 165412 (2017).
[14] J. L. McChesney, A. Bostwick, T. Ohta, T. Seyller, K. Horn, J. González, and E. Rotenberg, Phys. Rev. Lett. **104**, 136803 (2010).
[15] S. Ulstrup, M. Schüler, M. Bianchi, F. Fromm, C. Raidel, T. Seyller, T. Wehling, and P. Hofmann, Phys. Rev. B **94**, 081403(R) (2016).
[16] S. Link, S. Forti, A. Stöhr, K. Küster, M. Rösner, D. Hirschmeier, C. Chen, J. Avila, M. C. Asensio, A. A. Zakharov, T. O. Wehling, A. I. Lichtenstein, M. I. Katsnelson, and U. Starke, Phys. Rev. B **100**, 121407(R) (2019).
[17] P. Rosenzweig, H. Karakachian, D. Marchenko, K. Küster, and U. Starke, Phys. Rev. Lett. **125**, 176403 (2020).
[18] M. M. Scherer, Physics **13**, 161 (2020).
[19] C.-H. Park, F. Giustino, J. L. McChesney, A. Bostwick, T. Ohta, E. Rotenberg, M. L. Cohen, and S. G. Louie, Phys. Rev. B **77**, 113410 (2008).
[20] K. Gofron, J. C. Campuzano, A. A. Abrikosov, M. Lindroos, A. Bansil, H. Ding, D. Koelling, and B. Dabrowski, Phys. Rev. Lett. **73**, 3302 (1994); D. H. Lu, M. Schmidt, T. R. Cummins, S. Schuppler, F. Lichtenberg, and J. G. Bednorz, *ibid.* **76**, 4845 (1996).
[21] N. Tancogne-Dejean and A. Rubio, Phys. Rev. B **102**, 155117 (2020), and references therein.
[22] K. V. Emtsev, A. A. Zakharov, C. Coletti, S. Forti, and U. Starke, Phys. Rev. B **84**, 125423 (2011); J. Aprojanz, P. Rosenzweig, T. T. N. Nguyen, H. Karakachian, K. Küster, U. Starke, M. Lukosius, G. Lippert, A. Sinterhauf, M. Wenderoth, A. A. Zakharov, and C. Tegenkamp, ACS Appl. Mater. Interfaces **12**, 43065 (2020).

[23] G. Kotliar, S. Y. Savrasov, K. Haule, V. S. Oudovenko, O. Parcollet, and C. A. Marianetti, Rev. Mod. Phys. **78**, 865 (2006).

[24] X.-Y. Feng, H. Zhong, J. Dai, and Q. Si, arXiv:1605.02380.

[25] C. Lee, X. Wei, J. W. Kysar, and J. Hone, Science **321**, 385 (2008); N. Ferralis, R. Maboudian, and C. Carraro, Phys. Rev. Lett. **101**, 156801 (2008); M. L. Teague, A. P. Lai, J. Velasco, C. R. Hughes, A. D. Beyer, M. W. Bockrath, C. N. Lau, and N.-C. Yeh, Nano Lett. **9**, 2542 (2009); T. M. G. Mohiuddin, A. Lombardo, R. R. Nair, A. Bonetti, G. Savini, R. Jalil, N. Bonini, D. M. Basko, C. Galiotis, N. Marzari, K. S. Novoselov, A. K. Geim, and A. C. Ferrari, Phys. Rev. B **79**, 205433 (2009); N. N. Klimov, S. Jung, S. Zhu, T. Li, C. A. Wright, S. D. Solares, D. B. Newell, N. B. Zhitenev, and J. A. Stroscio, Science **336**, 1557 (2012).

[26] S.-M. Choi, S.-H. Jhi, and Y.-W. Son, Phys. Rev. B **81**, 081407(R) (2010).

[27] V. M. Pereira and A. H. Castro Neto, Phys. Rev. Lett. **103**, 046801 (2009); V. M. Pereira, A. H. Castro Neto, and N. M. R. Peres, Phys. Rev. B **80**, 045401 (2009); F. M. D. Pellegrino, G. G. N. Angilella, and R. Pucci, *ibid.* **84**, 195404 (2011); **81**, 035411 (2010); R. M. Ribeiro, V. M. Pereira, N. M. R. Peres, P. R. Briddon, and A. H. Castro Neto, New J. Phys. **11**, 115002 (2009).

[28] J. H. Warner, E. R. Margine, M. Mukai, A. W. Robertson, F. Giustino, and A.I. Kirkland, Science **337**, 209 (2012).

[29] B. Amorim, A. Cortijo, F. de Juan, A. G. Grushin, F. Guinea, A. Gutiérrez-Rubio, H. Ochoa, V. Parente, R. Roldán, P. San-José, J. Schiefele, M. Sturla, and M. A. H. Vozmediano, Phys. Rep. **617**, 1 (2016).

[30] J. M. Soler, E. Artacho, J. D. Gale, A. García, J. Junquera, P. Ordejón, and D. Sánchez-Portal, J. Phys.: Condens. Matter **14**, 2745 (2002).

[31] D. M. Ceperley and B. J. Alder, Phys. Rev. Lett. **45**, 566 (1980).

[32] N. Troullier and J. L. Martins, Phys. Rev. B **43**, 8861 (1991).

[33] H. J. Monkhorst and J. D. Pack, Phys. Rev. B **13**, 5188 (1976).

[34] M. Casartelli, S. Casolo, G. F. Tantardini, and R. Martinazzo, Phys. Rev. B **88**, 195424 (2013).

[35] L. Craco, Phys. Rev. B **77**, 125122 (2008).

[36] L. Craco and S. Leoni, Phys. Rev. B **100**, 115156 (2019).

[37] L. Craco, M. S. Laad, S. Leoni, and A. S. de Arruda, Phys. Rev. B **87**, 155109 (2013); L. Craco, S. S. Carara, T. A. da Silva Pereira, and M. V. Milošević, *ibid.* **93**, 155417 (2016); L. Craco and S. S. Carara, *ibid.* **101**, 205406 (2020).

[38] L. Craco and S. Leoni, Phys. Rev. B **85**, 075114 (2012); L. Craco, T. A. da Silva Pereira, S. R. Ferreira, S. S. Carara, and S. Leoni, *ibid.* **98**, 035114 (2018).

[39] Z. Qi, A. L. Kitt, H. S. Park, V. M. Pereira, D. K. Campbell, and A. H. Castro Neto, Phys. Rev. B **90**, 125419 (2014).

[40] L. Craco and G. Cuniberti, Appl. Phys. Lett. **85**, 3104 (2004); see also Braz. J. Phys. **32**, 293 (2002).

[41] A. K. Mitchell and L. Fritz, Phys. Rev. B **92**, 121109(R) (2015).

[42] M. Imada, A. Fujimori, and Y. Tokura, Rev. Mod. Phys. **70**, 1039 (1998).

[43] B. Irsigler, T. Grass, J.-H. Zheng, M. Barbier, and W. Hofstetter, arXiv:2011.05100.

[44] L. Craco, M. S. Laad, and E. Müller-Hartmann, Phys. Rev. Lett. **90**, 237203 (2003).

[45] L. Craco and M. A. Gusmão, Phys. Rev. B **52**, 17135 (1995).

[46] L. Ye, M. Kang, J. Liu, F. von Cube, C. R. Wicker, T. Suzuki, C. Jozwiak, A. Bostwick, E. Rotenberg, D. C. Bell, L. Fu, R. Comin, and J. G. Checkelsky, Nature (London) **555**, 638 (2018).

[47] H.-H. Lai, S. E. Grefe, S. Paschen, and Q. Si, Proc. Natl. Acad. Sci. USA **115**, 93 (2018).